



2004

First-principles study of magnetism in $(11\bar{2}0)$ $\text{Zn}_{1-x}\text{Mn}_x\text{O}$ thin film

Q. Wang

Virginia Commonwealth University

Puru Jena

Virginia Commonwealth University, pjena@vcu.edu

Follow this and additional works at: http://scholarscompass.vcu.edu/phys_pubs

 Part of the [Physics Commons](#)

Wang, Q., Jena, P. First-principles study of magnetism in $(11\bar{2}0)$ $\text{Zn}_{1-x}\text{Mn}_x\text{O}$ thin film. *Applied Physics Letters*, 84, 4170 (2004). Copyright © 2004 AIP Publishing LLC.

Downloaded from

http://scholarscompass.vcu.edu/phys_pubs/44

This Article is brought to you for free and open access by the Dept. of Physics at VCU Scholars Compass. It has been accepted for inclusion in Physics Publications by an authorized administrator of VCU Scholars Compass. For more information, please contact libcompass@vcu.edu.

First-principles study of magnetism in (11 $\bar{2}$ 0) Zn_{1-x}Mn_xO thin film

Q. Wang and P. Jena^{a)}

Department of Physics, Virginia Commonwealth University, Richmond, Virginia 23284

(Received 8 December 2003; accepted 30 March 2004; published online 6 May 2004)

First-principles calculations of total energies and magnetism of Zn_{1-x}Mn_xO thin film are performed by simulating it with a slab consisting of seven layers along (11 $\bar{2}$ 0). It is shown that a single Mn atom shows very little preference for the site it occupies. This is consistent with the experimental finding that Mn atoms are homogeneously distributed in ZnO films. As the concentration of Mn atoms increases, antiferromagnetic coupling between Mn atoms becomes more favorable, and there is a tendency for Mn atoms to form clusters around oxygen, in agreement with recent experiments.

© 2004 American Institute of Physics. [DOI: 10.1063/1.1755834]

The recent discovery of room temperature ferromagnetism in Mn-doped GaAs¹⁻³ has added a new dimension to the importance of this material. The *s*, *p* electrons of GaAs are responsible for transport, while the *d* electrons of Mn are responsible for the magnetic properties. Consequently, the coupling between these electrons can be exploited in new magnetic devices for information processing and data storage. This possibility has created much interest in the study of dilute magnetic semiconductors where transition metal atoms are doped into II-IV and III-V semiconductors. While most of the studies have concentrated on the III-V semiconductors, attention has recently been focused on the II-VI system such as (Zn, Mn)O.

ZnO is a wide-band-gap semiconductor with a direct gap of 3.4 eV. It has a wide range of applications in optical coatings, light emitting diodes, chemical sensors, and catalysts for hydrogenation/dehydrogenation reactions. Since the solubility of Mn in ZnO is much larger than that in GaN, great experimental efforts have been devoted to the study of magnetism in ZnO induced by Mn doping, especially for ZnO thin films. It is believed that the confined electrons or photons in such thin films are expected to exhibit outstanding properties and functionalities.

In this letter, we report calculations of total energies, electronic structure and magnetic properties of Mn-doped (11 $\bar{2}$ 0) ZnO thin film based on density functional theory and the generalized gradient approximation for exchange and correlation.⁴ This formalism has been successful in the past in predicting the magnetic moment of Mn₁₃ cluster by Nayak *et al.*,⁵ which has been recently confirmed by the magnetic deflection experiment of Knickelbein.⁶ Similarly the predicted electron affinity of MnO₄⁻ anion is in quantitative agreement with experiment.⁷

The (11 $\bar{2}$ 0) thin film was modeled by a slab of seven layers containing a total of 56 atoms. To preserve symmetry, the two top and bottom layers of the slab were taken to be identical, and each slab was separated from the other by a vacuum region of 10 Å. The central three layers were fixed at their bulk configuration, while the surface and subsurface layers on either side of the slab were allowed to relax without any symmetry constraint for all the calculations reported

in the following. The total energies, forces, and geometry optimizations were carried out using a plane-wave basis set with the projector augmented plane wave (PAW) method⁸ and the generalized gradient approximation for exchange and correlation,⁹ as implemented in the Vienna *ab Initio* Simulation Package (VASP).¹⁰ *k*-point convergence was achieved with a (6×4×1) Monkhorst-Pack¹¹ grid, and test with up to (8×6×2) Monkhorst *k*-points mesh were made. The energy cutoff was set at 350 eV and the convergence in energy and force were 10⁻⁴ eV and 3×10⁻³ eV/Å, respectively. To study the sensitivity of our results on the number of layers, calculations were repeated on slabs containing five, nine, and eleven layers (40, 72, and 88 atoms/supercell, respectively) for undoped ZnO slabs. The energy gain due to the surface relaxation was found to be 0.201, 0.234, 0.233, and 0.235 eV/dimer for five, seven, nine, and eleven layers, respectively. Similarly, the Zn-O lengths in the surface and subsurface also converged in seven-layer slab. Thus in the following we only discuss our results based on the seven-layer slab.

The geometry of the supercell containing 56 atoms (Zn₂₈O₂₈), which form zigzag ZnO dimer chains, is given in Fig. 1. The Zn-O dimer on the first layer is tilted by an angle of 7.48°. The O atoms on the first and second layer moved upward by 0.24 Å and downward by 0.04 Å along the [11 $\bar{2}$ 0] direction, respectively. Similarly the distances between the Zn and O atoms in the surface layer contracts by -5.5% and -5.8% along [1 $\bar{1}$ 00] and [0001], respectively. While the bond length between Zn on the first layer and O on the second layer contracts by only -1.6%, the corresponding relaxation between atoms in the second layer is much smaller. These results are in good agreement with the recent calculations of Meyer and Marx.¹² The energy gain due to relaxation is calculated by taking the difference between the total energies of the slabs before and after relaxation and dividing by the number of surface dimers that relaxed the most (there are four on each of the slab surfaces). We find this energy gain to be 0.23 eV/dimer.

In Fig. 2(a) we plot the total density of states for spin-up and spin-down electrons corresponding to undoped ZnO (11 $\bar{2}$ 0) film. Note that the densities of states for spin-up and spin-down electrons are identical and hence the film is non-magnetic.

^{a)}Electronic mail: pjena@vcu.edu

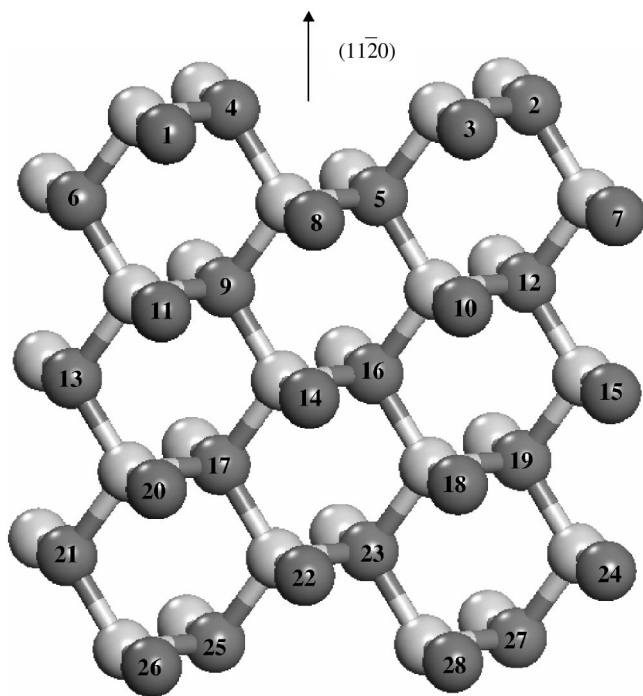


FIG. 1. Side view of the supercell of ZnO (11 $\bar{2}$ 0) slab consisting of 28 Zn and 28 O atoms. The numbered atoms are Zn.

The properties of Mn-doped ZnO were studied in successive steps. To determine the preferred site of Mn atoms, we first substituted a single Mn atom in a surface site (marked No. 4) and then in a subsurface site (marked No. 5) in Fig. 1. To preserve symmetry, we also replaced Zn sites in the bottom two layers of the slab, namely Nos. 25 and 23

with Mn, respectively. This led to a supercell consisting of Zn₂₆Mn₂O₂₈ and a Mn concentration of 7.14%. We consider this concentration to be dilute as the distance between the two Mn atoms on the two sides of the slab is large and the interaction between the Mn atoms is expected to be weak. After optimization, the Mn–O bonds in the surface layer contract by –1.62% and –3.16% along [1 $\bar{1}$ 00] and [0001], respectively, while the bond between surface Mn and nearest subsurface O expands by 2.33%.

The energy gained by replacing the Zn atom with Mn is calculated by using the following equation:

$$\Delta \epsilon = -[E(\text{Zn}_{28-n}\text{Mn}_n\text{O}_{28}) - E(\text{Zn}_{28}\text{O}_{28}) + nE(\text{Zn}) - nE(\text{Mn})]/n, \tag{1}$$

where E is the total energy. The energy gains associated with Mn occupying the surface and subsurface sites are, respectively, 2.27 and 2.20 eV. Since this energy difference, namely 0.07 eV, is within the error of our calculation, we can assume that Mn atoms show no site preference. Thus, in the dilute limit, when Mn atoms are expected to be far apart, Mn can substitute Zn sites homogeneously. This confirms the experimental finding in the dilute limit.¹³ This is in contrast to (Ga, Mn)N where Mn occupying the surface site lies 1.37 eV lower than that occupying the subsurface site.¹⁴

We next discuss the magnetic coupling between two Mn atoms by replacing two Zn sites with Mn atoms. There are many ways this substitution can be achieved, depending upon which Zn sites are replaced by Mn. We have studied five different configurations. First, we have replaced two nearest neighbor Zn atoms by Mn on the surface layer marked Nos. 1 and 4 in Fig. 1 (configuration I). To preserve

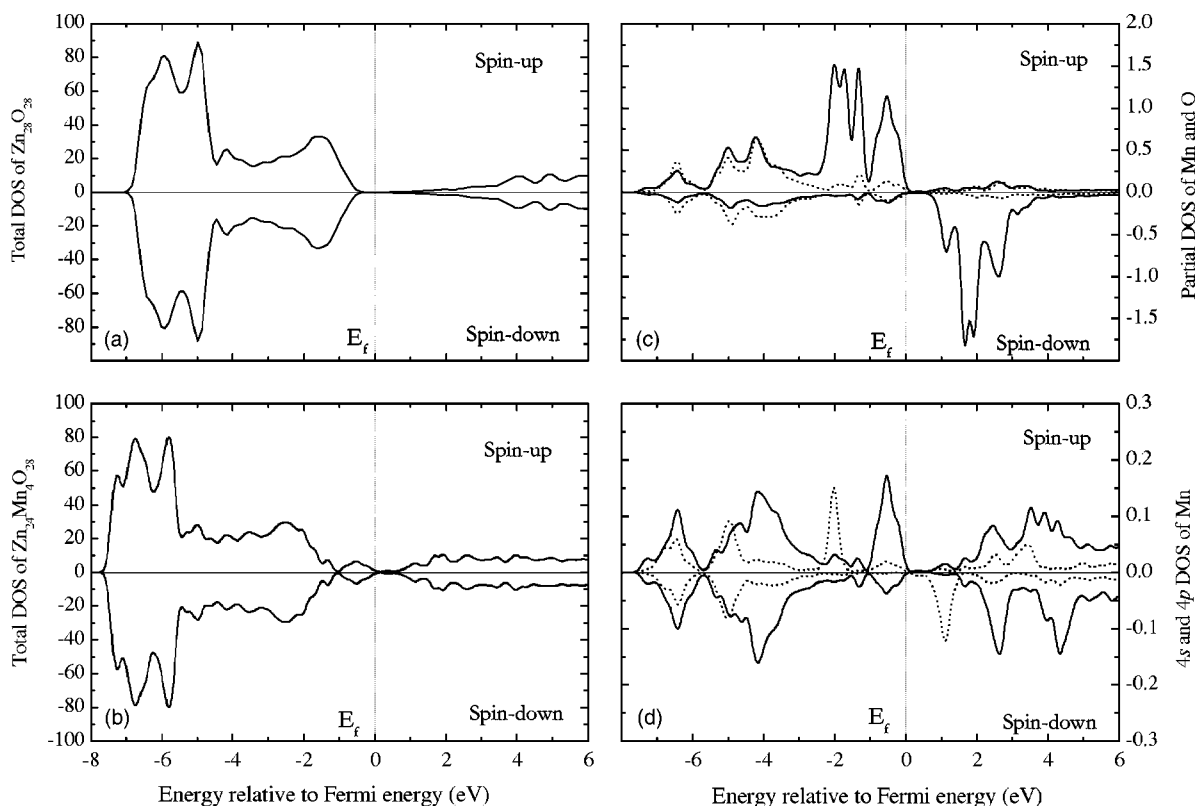


FIG. 2. Total spin density of states (DOS) for (a) Zn₂₈O₂₈; (b) Mn-doped ZnO (Zn₂₆Mn₂O₂₈); (c) partial spin DOS of Mn 3d (solid line) and O 2p (dotted line); (d) partial spin DOS of Mn 4s (dotted line) and 4p (solid line) in Zn₂₄Mn₄O₂₈.

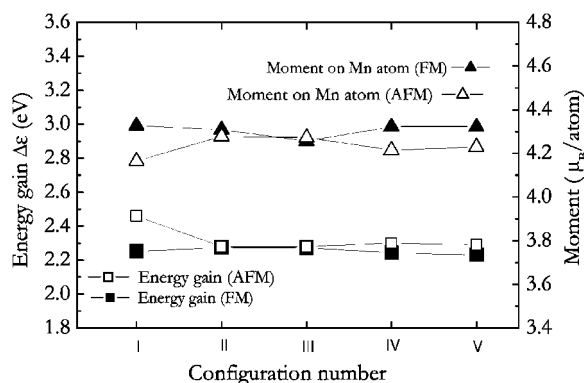


FIG. 3. Magnetic moments and energy gain in Mn doped ZnO thin film corresponding to antiferromagnetic (AFM) and ferromagnetic (FM) states for different configurations of Mn in $\text{Zn}_{28}\text{Mn}_4\text{O}_{28}$ supercell.

symmetry, we also replaced Zn at sites Nos. 26 and 25 with Mn. This corresponds to a $\text{Zn}_{24}\text{Mn}_4\text{O}_{28}$ supercell and a Mn concentration of 14.28%. In configuration II, Zn atoms on the sites of Nos. 2, 4, 25, and 27 are replaced by Mn atoms. Configuration III corresponds to the replacement of sites Nos. 1, 2, 26, and 27. Configuration IV relates to the substitution of two Zn sites by Mn with one in the surface layer and the other in the subsurface layer. This has Mn atoms substituting Zn at sites Nos. 2, 5, 27, and 23. Configuration V corresponds to the substitution of Zn atoms at the subsurface layer at sites Nos. 5, 8, 23, and 22. Typically, the Mn–O distance in the surface layer (configuration I) relaxes by -4.11% and -4.66% along $[1\bar{1}00]$ and $[0001]$, while that of the nearest Mn–O distance on the second layer relaxes about 0.91% . The relaxed Mn–Mn distances for configurations I, II, III, IV, and V are 2.91, 5.62, 7.78, 3.21, and 3.17 Å, respectively. The studies of the total energies of these configurations can not only yield the preferred distance between the Mn atoms, but also can illustrate how the magnetic coupling changes with Mn–Mn distance.

We have calculated the energy gain per Mn atom for the above five configurations by using Eq. (1) for both ferromagnetic and antiferromagnetic spin alignments. These results are given in Fig. 3. The lowest energy configuration (I) is an antiferromagnetic state where Mn atoms replace the two nearest Zn sites in the surface layer. This suggests that Mn atoms have a tendency to form clusters around oxygen, in agreement with the recent experiment¹⁵ on an epitaxial Zn–MnO thin film fabricated with a laser molecular-beam method. In the ground state configuration I of (Zn, Mn)O, the ferromagnetic (FM) state lies 0.21 eV/Mn atom above the antiferromagnetic (AFM) state. This agrees with experiment¹⁶ where the authors did not observe FM behavior. On the contrary, an AFM interaction between Mn atoms is experimentally identified in Mn-doped ZnO system.^{17,18}

The total density of states (DOS) corresponding to configuration I is shown in Fig. 2(b). Note that the densities of states for spin-up and spin-down states are again identical leading to zero magnetic moment. This is to be expected in

an AFM system. However, the energy gap is considerably reduced from that in undoped ZnO [see Fig. 2(a)]. The magnetic moment of each Mn atom is $4.17 \mu_B$ and mainly arises from the Mn 3d orbital ($3.93 \mu_B$). Due to the *sp* and *d* hybridization, small contributions to the moment also comes from 4*s* ($0.13 \mu_B$) and 4*p* orbitals ($0.10 \mu_B$) of Mn. The hybridization between O 2*p* and Mn 3*d* [as shown in Fig. 2(c)] reduces the magnetic moment as compared to that of a free Mn atom. Figure 2(d) shows the partial spin DOS of Mn 4*s* and 4*p* in $\text{Zn}_{24}\text{Mn}_4\text{O}_{28}$.

It is interesting to note the changes in energy difference between AFM and FM states for different geometry configurations. The energy difference nearly vanishes in configurations of II and III, as shown in Fig. 3. Note that for these two configurations, the Mn atoms are 5.62 and 7.78 Å apart and the large distances result in very weak magnetic coupling. Therefore, the energy difference between FM and AFM states should be very small.

In summary, we have investigated the electronic structure and magnetism of Mn-doped ZnO thin film in detail using first-principles calculations. It is found that in the $\text{Zn}_{1-x}\text{Mn}_x\text{O}$ thin film the clustering of Mn atoms around O takes place at higher Mn concentrations, and the magnetic coupling between Mn ions is antiferromagnetic. This is in agreement with the recent calculation of Sato and Katayama-Yoshida of a Mn-doped ZnO crystal.¹⁹ Because Mn and Zn have the same valence, there are no free holes to mediate ferromagnetism when Mn atoms substitute at Zn sites. To obtain ferromagnetism in this system, other treatments, such as codoping and defects, are needed.²⁰

This work was partly supported by a grant from the Office of Naval Research. The authors are thankful to Dr. A. K. Rajagopal and Professor H. Morkoç for interesting discussions.

- ¹T. Dietl, H. Ohno, F. Matsukura, J. Cibert, and D. Ferrant, *Science* **287**, 1019 (2000).
- ²H. Ohno, *Science* **281**, 951 (1998).
- ³H. Ohno, *Science* **291**, 840 (2001).
- ⁴J. P. Perdew and Y. Wang, *Phys. Rev. B* **45**, 13244 (1992).
- ⁵S. K. Nayak, M. Nooijen, and P. Jena, *J. Phys. Chem. A* **103**, 9853 (1999).
- ⁶M. B. Knickerbein, *Phys. Rev. Lett.* **86**, 5255 (2001).
- ⁷G. L. Gutsev, B. K. Rao, P. Jena, X.-B. Wang, and L.-S. Wang, *Chem. Phys. Lett.* **312**, 598 (1999).
- ⁸P. E. Bloechl, *Phys. Rev. B* **50**, 17953 (1994).
- ⁹J. P. Perdew and Y. Wang, *Phys. Rev. B* **45**, 13244 (1992).
- ¹⁰G. Kresse and J. Heffner, *Phys. Rev. B* **54**, 11169 (1996).
- ¹¹H. J. Monkhorst and J. D. Pack, *Phys. Rev. B* **13**, 5188 (1976).
- ¹²B. Meyer and D. Marx, *Phys. Rev. B* **67**, 035403 (2003).
- ¹³X. M. Cheng and C. L. Chien, *J. Appl. Phys.* **93**, 7876 (2003).
- ¹⁴Q. Wang, Q. Sun, and P. Jena (unpublished).
- ¹⁵Z. Jin, Y.-Z. Yoo, T. Sekiguchi, T. Chikyow, H. Ofuchi, H. Fujioka, M. Oshima, and H. Koinuma, *Appl. Phys. Lett.* **83**, 39 (2003).
- ¹⁶K. Ueda, H. Tabata, and T. Kawai, *Appl. Phys. Lett.* **79**, 988 (2001).
- ¹⁷T. Fukumura *et al.*, *Appl. Phys. Lett.* **78**, 958 (2001).
- ¹⁸S. W. Yoon, S.-B. Cho, S. C. We, S. Yoon, B. J. Suh, H. K. Song, and Y. J. Shin, *J. Appl. Phys.* **93**, 7879 (2003).
- ¹⁹H. Katayama-Yoshida and K. Sato, *J. Phys. Chem. Solids* **64**, 1447 (2003).
- ²⁰K. Sato and H. Katayama-Yoshida, *Jpn. J. Appl. Phys., Part 2* **39**, L555 (2000).